Technische Universität München

Technische Universität München
Fakultät für Elektrotechnik und Informationstechnik
Professur für Computational Photonics
Prof.Dr.-Ing. Christian Jirauschek

Coupled Transmission Line/Maxwell-Bloch Equations Approach for Electro-Optical Simulations of Terahertz Quantum Cascade Lasers

MASTER THESIS

by Longwei Zhong

April, 2017

Abstract

Quantum cascade lasers (QCLs) are compact, electrically pumped semiconductor devices, which are considered to be promising light sources for far- and mid-infrared regions. Despite its practical significance, generating ultra short pulses from QCLs by mode-locking has achieved only limited success.

There are already several successful experimental attempts by active mode locking so far, but a complete theory system is still not available due to limited knowledge of quite complex mechanism inside cavity, both electrical as well as optical. The purpose of this research is to build a new model based on existed simulation methods to achieve a dynamic modeling of QCLs in time domain, which would help to get a better understanding of its theoretical mechanism and redound to still unresolved issues of the field.

Acknowledgements

Thanks to Petar

I dedicate this work to my beloved mother and father

List of Symbols

Contents

1 Introduction

QCLs have gained considerable attention since they were first demonstrated at Bell Laboratories in 1994 by Jerome Faist and his colleagues[1]. Due to lack of suitable radiation sources and detectors this region remains one of the least developed spectral regions. Unlike common semiconductor lasers, which utilize electron-hole recombination to realize electromagnetic radiation, QCLs are based on intersub- band transitions in coupled quantum well superlattices[2]. Benefit from this special mechanism QCLs can utilize the electric power more efficiently and achieve a high output power.

Mode-locking is a technique in optics, which locks multi-mode in resonant laser cavity by enforcing coherence between modes to produce extra short pulse[5]. Methods of mode-locking can be simply classified in active mode-locking (AML) and passive mode-locking(PML) depending on whether it is modulated by itself (e.g. absorber) or requires external modulation source (e.g. RF source).

1.1 Background and Motivation

It has been proven to be difficult to directly employ existing techniques from the ultra fast optics community to mode-lock QCLs due to unfavorable physical effects and lack of consolidation theory about its mechanism. Despite various obstacles some clear mode-locking of QCLs has been realized already in the mid-infrared as well as terahertz. All of the attempts are based on active mode-locking, which was recognized as the only viable route to QCL mode locking [6]. The main idea is to actively mode-lock the QCLs through a modulated injection current with a frequency corresponding to the round-trip frequency f_{rt}, which lies in the microwave region extending from around 3 kHz to 300 GHz.

The first successful attempt in mid-IR QCLs was achieved in 2009 [4] by modulating a short section of the cavity to open a net gain window. Different with common QCL design (Bound to continuum, Chirped superlattice, Resonant-phonon, Hybrid/interlaced), the QCL that was used is based on a "diagonal transition", which was a specially designed and owns significant longer gain recovery time. It was found that mode-locked pulses can be formed by modulating current injection close to the laser threshold, while high above threshold pulses are broadened due to multi-mode instabilities (Spatial Hole Burning and RNGH-instability).

Recently active mode locking of QCLs in an external ring cavity was reported [6], which can operate at room temperature. Moreover, benefits from this method, the mode-locking was observed not only at close to the threshold, but also far above it.

Similar to mode-locking in mid-IR, THz QCLs can also be injection locked by active mode-locking with an external RF source. Besides, it was found that mode-locking in THz QCLs is easier than that in mid-IR. Compared with mid-IR QCLs, the laser transition energy lies below the optical phonon energy, so the upper state of THz QCLs based on bound-to-continuum has generally longer non-radiative relaxation time ($\sim$ 5-10 ps), which makes it easier to mode-lock [7]. The first successful attempt of mode-locking in THz QCLs was reported in 2010 [8]. The same with in mid-IR QCLs, they also used RF modulation to achieve mode-locking with a modulation frequency corresponding to the round trip frequency of the laser. By direct amplitude modulation, the mode-locking of a 2.3THz QCL was achieved at 35GHz with input RF-power <-15dBm.

In the last two decades many studies have been carried out on further development as well as possible applications of QCLs. Some groups devoted themselves to improve the operation temperature, up to room temperature has been achieved[3] through special wells design of QCL structure. Some consisted on generating short pulse by using QCLs[4]. Besides, In the past few years researchers have showed high interest in the application of QCLs. There are already many ....

1.2 Related work

different models, advantage and drawbacks

1.3 Objective

The objectives of this thesis are as follows:

1). To build a new dynamic model

2). To verify "pulling effect" in mode-locking through simulation

3). To acquire optimal simulation parameters to generate short pulse

4). To gain a deep understanding of mode-locking behaviors to obtain a better design in the future.

2 Optical Modeling

Similar with the existing modeling methods, in this model light propagation is described with Maxwell' equation while carrier transportation is determined by Bloch equation. Without regard to lateral non-uniform distribution at boundaries [9, 10] QCL can be simplified to one-dimensional (1D) structure in the direction of propagation (x axis), which means the electrical components were uniformly distributed throughout the cross-sectional area.

2.1 Light Propagation

2.2 Carrier Transport

3 Electrical Modeling

In the electrical modeling, a modified Transmission Line Method (TLM) was introduced in order to realize a dynamic modeling in time domain. TLM is a very efficient methode which is already widely used for evaluation and dynamic modeling, for example, contact resistance extraction in organic field- effect transistors [11], dynamic modeling of flow in pipelines [12] etc. However, TLM is specially for analysis of transverse electromagnetic (TEM) modes while in QCLs are transverse magnetic (TM) modes [13]. The common used metal-metal waveguide (microstrip structure) in QCLs can be regarded as quasi-TEM structure, if the substrate ($\sim$ 10 um) is thin in terms of wavelength (30 mm $\sim$ 300 mm), and if the strip conductor is very narrow ($\sim$ 50 um) in terms of wavelength, then a static analysis should be perfectly adequate.

3.1 Transmission Line Method

The conventional TLM is described by Telegrapher's equations (3.1)(3.2) with distributed components (distributed resistance R', istributed inductance L', distributed capacitance C', distributed conductance G'). The distributed resistance R' of conductors is represented by a series resistor and expressed in ohms per unit length. The distributed inductance L' results from the magnetic field around the line due to self-inductance which is represented by a series inductor (in henries per unit length). The distributed conductance G' (siemens per unit length) of the dielectric material separating the two conductors is represented by a shunt resistor, which has a resistance of 1/G'.

Depending on characteristics of line and medium it can also be further classified in lossy/non-lossy transmission line and uniform/nonuniform transmission line. When no resistance and conductance exist, it can be regarded as ideal transmission line which contains only L' and G'. Besides, both of them are uniformly distributed along line. Under the assumptions above in optical modeling the simulated QCL should be a 1D nonlinear lossy transmission line.

Telegrapher's equations:

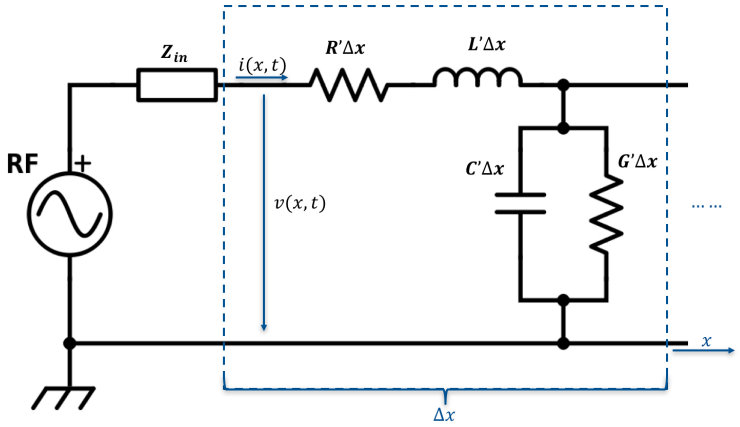

Figure 3.1: *: An equivalent circuit representation of a differential section of the waveguide with capacitance per unit length C′ and inductance per unit length L′.*

$$\frac{\partial v(x,t)}{\partial x} = -L'\frac{\partial i(x,t)}{\partial t} - R'i(x,t) \tag{3.1}$$

$$\frac{\partial i(x,t)}{\partial x} = -C'\frac{\partial v(x,t)}{\partial t} - G'v(x,t) \tag{3.2}$$

In this modeling, the vertical current component due to distributed conductance G′ will be replaced by current density J(x,t) which is nonuniform bias dependent and will be obtained by carrier transmission in optical part. In order to solve these two partial differential equations, finite difference in time domain (FDTD) method was applied. This method is widely used to solve transmission line problem in time domain and has second order accuracy.

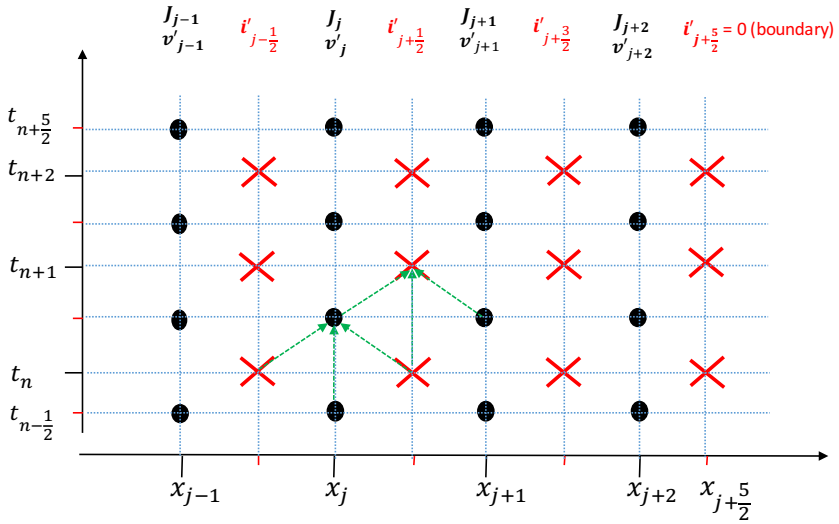

Figure 3.2: *Discretization along a staggered temporal and spatial grid.*

Following Yee's staggered grid approximation[14], voltage and current are discretized with separation of $\Delta x/2$ and $\Delta t/2$ in space and time respectively (See Figure 3.2), which leads to a second-order accurate approximation. Voltage V(x,t) and current I(x,t) samples are then expressed as $V\big(j\Delta x, (n+\frac{1}{2})\Delta t\big)$ and $I\big((j+\frac{1}{2})\Delta x, n\Delta t\big)$, where j and n are integers. For reasons of simplicity, in the following text they will be replaced with $V_j^{n+\frac{1}{2}}$ and $I_{j+\frac{1}{2}}^n$. After discretization, the first-order derivative of voltage $\partial V(x,t)$ as well as current $\partial I(x,t)$ in space and time can be simply calculated with central difference method[15].

In this way the original Telegrapher's equations (3.1) and (3.2) are constructed as:

$$\frac{V_{j+1}^{n+\frac{1}{2}} - V_j^{n+\frac{1}{2}}}{\Delta x} \approx -L' \frac{I_{j+\frac{1}{2}}^{n+1} - I_{j+\frac{1}{2}}^n}{\Delta t} - R' \tilde{i}_{j+\frac{1}{2}}^{n+\frac{1}{2}} \tag{3.3}$$

$$\frac{I_{j+\frac{1}{2}}^n - I_{j-\frac{1}{2}}^n}{\Delta x} \approx -C' \frac{V_j^{n+\frac{1}{2}} - V_j^{n-\frac{1}{2}}}{\Delta t} - w J_j^n \tag{3.4}$$

where, $\tilde{i}_{j+\frac{1}{2}}^{n+\frac{1}{2}}$ is the ac (alternating current) component at node j due to external RF source and w denotes width of simulated laser cavity. The ac component plays a role especially in high frequency case, in which metal shows high resistance due to RF source. However, during simulation it's not possible to separate ac component with high frequency from whole current. Instead, it will be approximately replaced with current different between adjacent time steps. Besides, the last terms of equation (3.3) has to be averaged in time for sake of consistence, the same with J_j^n, leading to:

$$(\frac{L'}{\Delta t} + \frac{R'}{2}) I_{j+\frac{1}{2}}^{n+1} \approx -\frac{V_{j+1}^{n+\frac{1}{2}} - V_j^{n+\frac{1}{2}}}{\Delta x} + (\frac{L'}{\Delta t} + \frac{R'}{2}) I_{j+\frac{1}{2}}^n \tag{3.5}$$

Subsequently, after rearrangement a recursive solution for Transmission line updating are explicitly expressed as:

$$I_{j+\frac{1}{2}}^{n+1} = I_{j+\frac{1}{2}}^n - (\frac{L'}{\Delta t} + \frac{R'}{2})^{-1} \frac{V_{j+1}^{n+\frac{1}{2}} - V_j^{n+\frac{1}{2}}}{\Delta x} \tag{3.6}$$

$$V_j^{n+\frac{1}{2}} = V_j^{n-\frac{1}{2}} - \frac{\Delta t}{C'\Delta x}\big(I_{j+\frac{1}{2}}^n - I_{j-\frac{1}{2}}^n + w\Delta x \frac{J_j^{n+\frac{1}{2}} + J_j^{n-\frac{1}{2}}}{2}\big) \tag{3.7}$$

3.1.1 Boundary Conditions

Boundary conditions account for the completeness of differential equations at the boundary. In this case, the right side of QCL lefts open, so no current exists. Consequently, the boundary condition for current is $I_{end}^n = 0$.

QCL was supplied with source V_S which consists of a DC voltage source V_{DC} and an external RF source V_{RF}, therefore $V_S = V_{DC} + V_{RF}$. But due to existance of wire

impedance the voltage at node 0 is not equal to source voltage V_S. Besides, a cascading of π networks[16] is introduced for the distributed transmission line by splitting the shunt capacitance and conductance in half with two parallel capacitors and conductors at boundary, which is illustrate in Fig. 3.3.

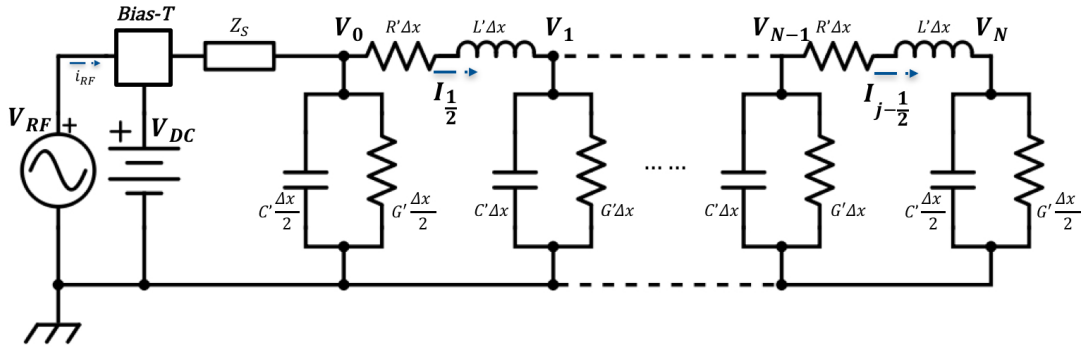

Figure 3.3: *Schematic of cascade π network representation and Thévenin equivalent circuit.*

By using Kirchhoff's voltage law (KVL), $V_{RF}^n + V_{DC} = Z_S \widetilde{i}^n_{-\frac{1}{2}} + V_0^n$, where $\widetilde{i}^n_{-\frac{1}{2}}$ denotes ac component among whole current after bias-T, which is relevant to current transmission from both RF and DC source. However, that cannot directly obtained through Fourier Transformation during iterative process. Thanks for the ultra short time step, $\widetilde{i}$ can be approximately replaced by corresponding current variation ΔI near node 0, leading to:

$$V_{RF}^n + V_{DC} = Z_S(I_{\frac{1}{2}}^n - I_{\frac{1}{2}}^{n-1} + C'\frac{\Delta x}{2}\frac{V_0^{n+\frac{1}{2}} - V_0^{n-\frac{1}{2}}}{\Delta t}) + \frac{V_0^{n+\frac{1}{2}} + V_0^{n-\frac{1}{2}}}{2} \tag{3.8}$$

Then the equation above is rearranged to get an explicit update expression at boundary:

$$V_0^{n+\frac{1}{2}} = \frac{Z_S C'\Delta x - \Delta t}{Z_S C'\Delta x + \Delta t} V_0^{n-\frac{1}{2}} + \frac{2\Delta t}{Z_S C'\Delta x + \Delta t}[V_{RF}^n + V_{DC} - Z_S(I_{\frac{1}{2}}^n - I_{\frac{1}{2}}^{n-1})] \tag{3.9}$$

3.1.2 Initial Conditions

Adequate initial conditions play a important role as well as boundary conditions to acquire an accurate solution. However, it is really hard to determine and verify the real electrical distribution of a laser at the very beginning. Here the following initial conditions are defined:

$$V_1^0 = V_2^0 = ... = V_j^0 ... = V_N^0 = V_{DC} \tag{3.10}$$

$$I_{j+\frac{1}{2}}^0 = I_S^0 \times \frac{N-j}{N} \quad (j = 0, 1, 2..., N-1) \tag{3.11}$$

where, I_S is the initial current injection in case no lasing, which can be obtained by integrating J(x,0) over x from optical model. N is the amount of nodes while j integer ranging from 0 to N-1. The initial condition for current is under assumption that at very beginning the current was linearly distributed along cavity in x direction.

3.2 Modulation Power

Not only modulation frequency but also modulation power plays a key role in mode-locking. Even if QCL was modulated at near round trip frequency f_{rt} , it can't be mode locked without enough modulation power. So it is essential to figure out RF power for each simulation in order to analyze the modulation process.

Two methods to estimate modulation power:

1. Through Fourier Transformation ac component can be easily separated at modulation frequency f_{RF} from recorded whole current data over time. In the way, average RF voltage signal can also be obtained. Therefore, the injected RF-power to QCL is approximately:

$$P_{RF} = \delta I * \delta V \tag{3.12}$$

where δI and δV are current and voltage component at f_{RF}, respectively.

2. Using the formula [17], which is used for calculation of small signal current modulation:

$$P_{diss} = \frac{\delta I_{QCL}^2 * Re[Z_{QCL}]}{2} \tag{3.13}$$

where, δI_{QCL} is induced current variation due to RF source and Z_{QCL} is the impedance of QCL at modulation frequency.

3.3 Estimation of Distributed Components

The involvement of transmission line requires distributed component parameters. Except for distributed conductance G', which will be calculated in optical part, distributed resistance R', distributed inductance L' as well as distributed capacitance C' still need to be determined. They can be either calcuted as convertial passive components (plane resistor, parallel plane capacitor and inductor), or extracted from S-Parameter, which can be directly measured with network analyser. The former methode is simple and also don't require any extra test, but could lead to large error due to neglection of fringe effect[18] as well as high frequency influence. The latter is based on experiment, so shows higher accuracy compared with former, but requires extra experiment as well as equipment, which is not always feasible for simulation research.

Distributed resistance is frequency dependent and can be obtained by measurement of S-parameter [19], which shows constant value when under certain frequency $R' = 4.5 \times 10^{-5}\sqrt{f_{RF}}$ /mm.

3.3.1 Distributed Capacitance

The cavity of QC laser is regarded as microstrip line in this case. Quasi-TEM structures, like microstrip, will have frequency dependent impedance and effective dielectric constant. However, if the substrate ($\sim$ 10 um) is thin in terms of wavelength (30 mm $\sim$ 300 mm), and if the strip conductor is very narrow ($\sim$ 50 um) in terms of wavelength, then a static analysis should be perfectly adequate.)

Numerically, one only have to consider a small, bounded 2D region with assumption of uniform cross-section going into the page (See Figure 3.5).

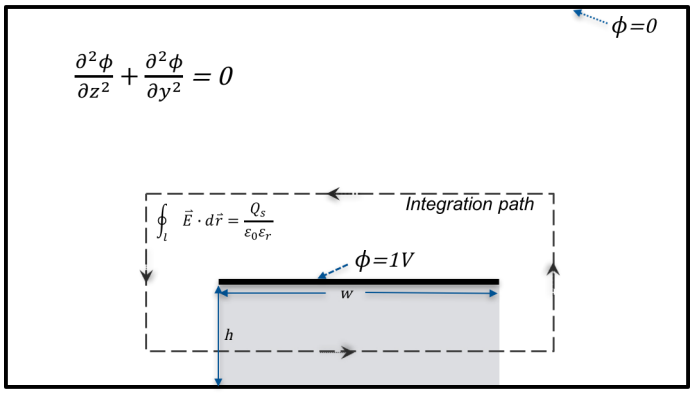

Figure 3.4: *Gauss's 2D equation.*

The electric field can be solved by Gauss's law in 2D. Solving for a strip in a box (Figure 2) the strip potential was set to 1V, the boundary to 0V and solve for the potential at a number of points inside the box. Here an electromagnetic field-solver QuickField was used which is a stand-alone software for solving partial differential equation (PDE). Figure 3 shows the calculated electric field around the strip.

$$\frac{\partial^2\phi}{\partial y^2} = \frac{\phi_{i-1,j} - 2\phi_{i,j} + \phi_{i+1,j}}{(\Delta y)^2} \tag{3.14}$$

$$\frac{\partial^2\phi}{\partial z^2} = \frac{\phi_{i,j-1} - 2\phi_{i,j} + \phi_{i,j+1}}{(\Delta z)^2} \tag{3.15}$$

Set $\Delta y = \Delta z = \Delta$, then spacial electrical potential at each grid except top metal layer inside box can be resolved $\phi_{i,j} = \frac{\phi_{i-1,j}+\phi_{i+1,j}+\phi_{i,j-1}+\phi_{i,j+1}}{4\Delta^2}$

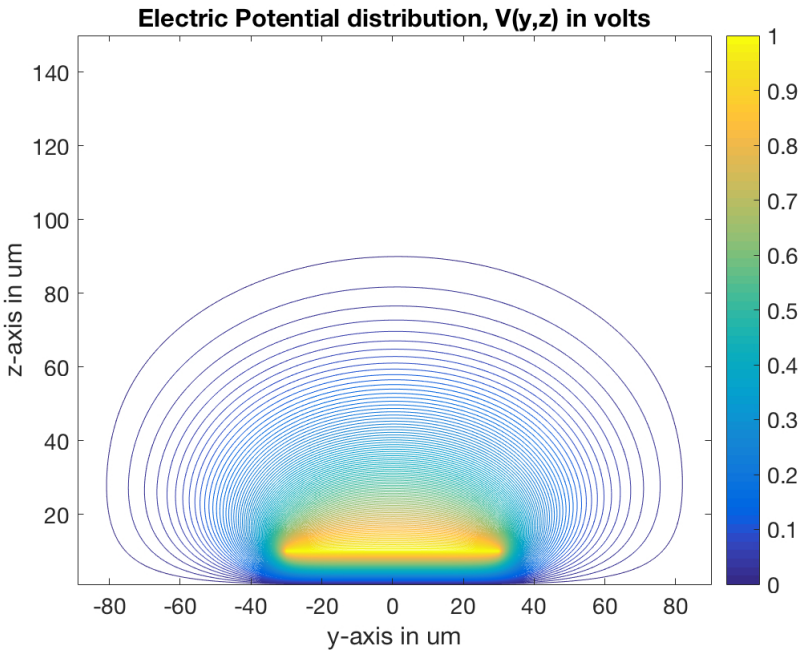

Figure 3.5: *Calculated electrical potential distribution V(y,z) with Matlab.*

$E = -\nabla\phi$

pictures and calculations...

$Q_S = \oint_l \varepsilon_0 \varepsilon_r \overrightarrow{E} \cdot d\overrightarrow{r}$

3.3.2 Distributed Inductance

Ampere's circuital law

$$\nabla \times H = J \tag{3.16}$$

$$\frac{\partial H}{\partial y} - \frac{\partial H}{\partial z} = J \tag{3.17}$$

$$\mathbf{H}_P = \sum_{i=1}^{n} \sum_{j=1}^{n} \frac{\mathbf{I} \times \mathbf{R}_{i,j} \Delta S}{4\pi R_{i,j}^3 w} \tag{3.18}$$

where, w is width of lateral cross section and R is vector pointing from the surface element to the observation point P.

The magnetic field at a point $\mathbf{H}_P$ results from the magnetic field of each surface element, and can be calculated by adding all these together.

...

The energy of inductor $W = \frac{1}{2}LI^2 = \frac{1}{2}\int_{\Omega} BHd\Omega$

pictures and calculation.... use the function quiver of Matlab to plot our vector plot.

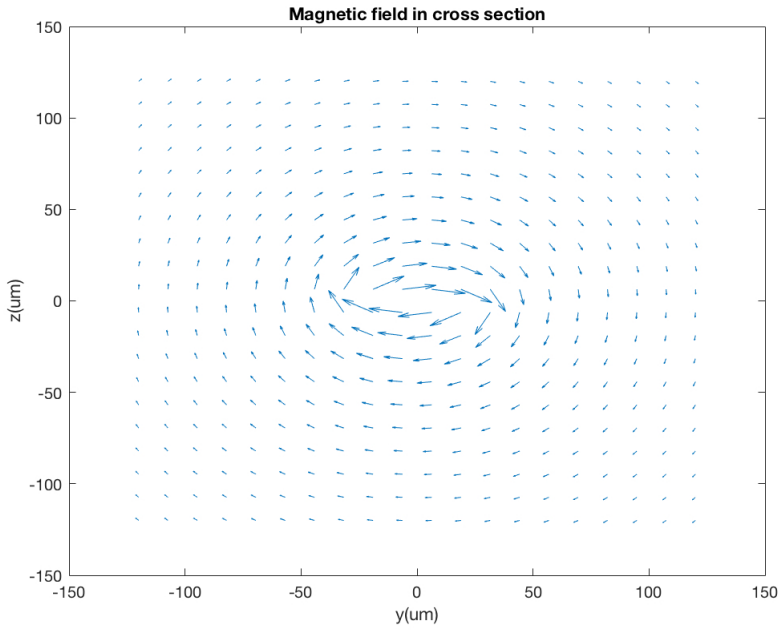

Figure 3.6: *Magnetic feld in cross section y-z plane.*

4 Simulation Results and Comparison with Experiment

The simulated laser is ...QCL structure...

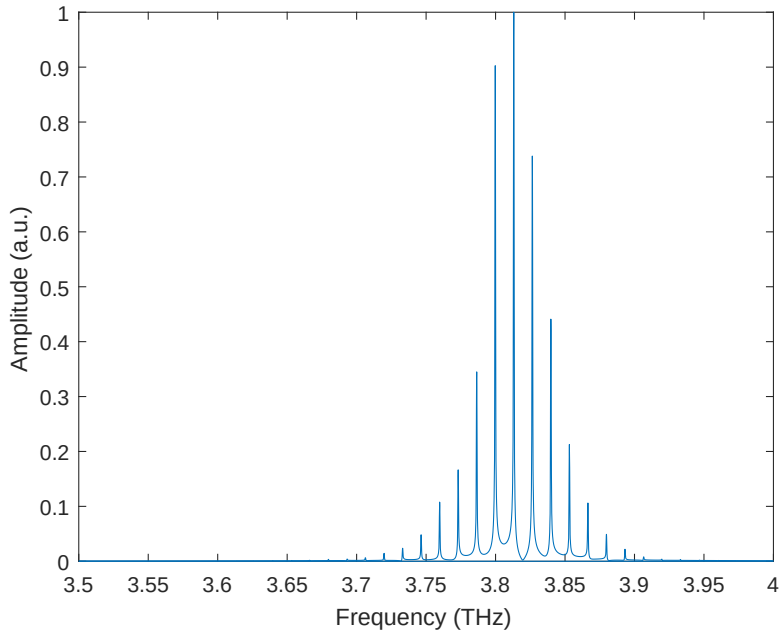

Figure 4.1: *laser spectrum.*

Round trip frequency f_{rt} is 13.34 GHz.

add I-V curve from Petar

4.1 Simulation Setup

The source of simulated QCL consists of a DC voltage source and a RF source, which are combined through bias-T.

replace this ugly picture with that from petar

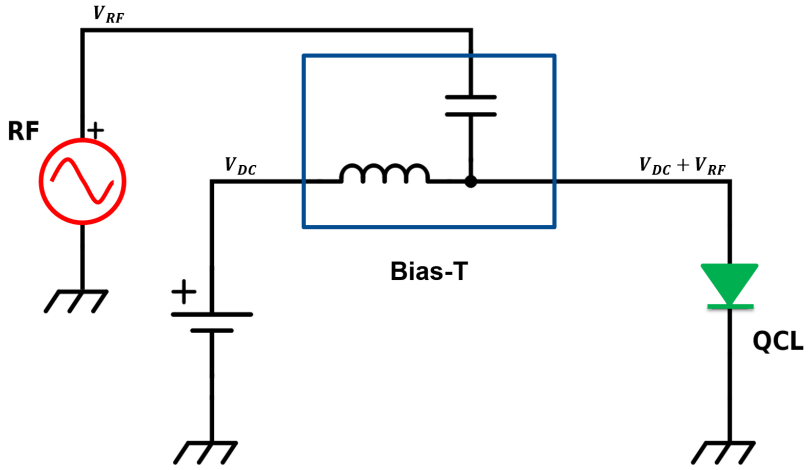

Figure 4.2: *schematic scheme.*

Table 4.1: *Simulation parameters*

Name	Symbol	Value	Unit
Cavity length	L_{tot}	3	mm
Cavity width	w	60	um
Doping density	D_p	1.5E16	cm^{-3}
Period length	L_p	54.8	nm
Overlap factor	Γ	0.8	
Cavity loss	L_α	13	$1/cm$

4.2 Simulation Results

After 100 round trips simulation, a clear short pulse was observed, as Figure 4.3 shows, from 4610 to 4690 ps in corresponding to 164 T_{rt}. Its Full Width at Half Maximum (FWHM) in this modeling is around 11.6 ps, which shows extremely good agreement with experiment result 11 ps[8].

4.3 Comparison with Experiment

Describe and argue this simulation results with experiment results from paper "Generating ultrafast pulses of light from qcls"

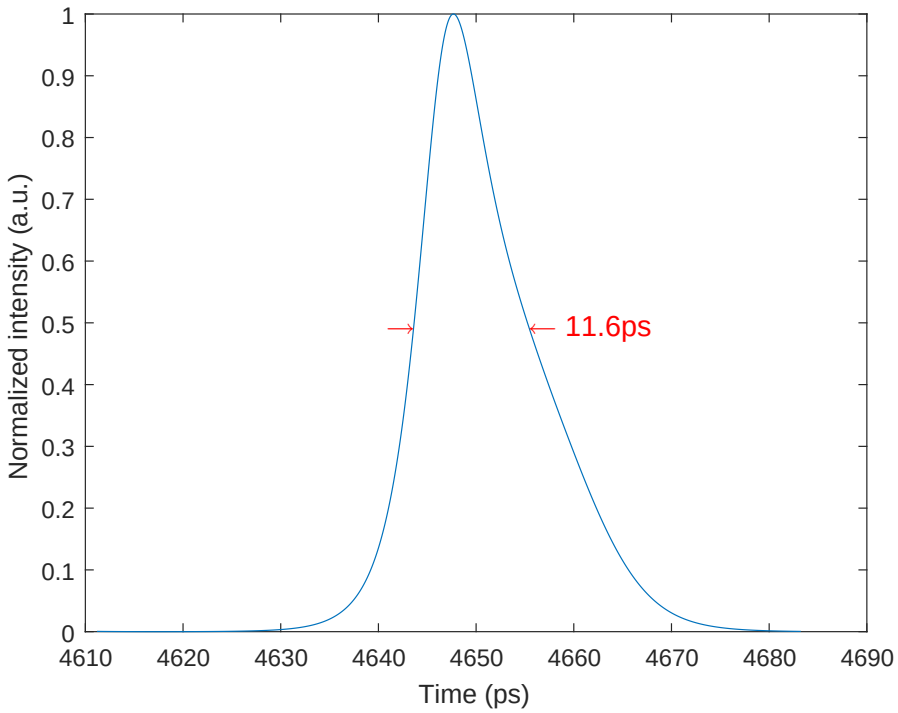

Figure 4.3: *Singel pulse from simulation.*

5 Conclusion

Bibliography

[1] J. Faist, F. Capasso, D. L. Sivco, C. Sirtori, A. L. Hutchinson, and A. Y. Cho, "Quantum cascade laser," *Science*, vol. 264, no. 5158, pp. 553–556, 1994. *Cited on page 1.*

[2] B. S. Williams, "Terahertz quantum-cascade lasers," *Nature photonics*, vol. 1, no. 9, pp. 517–525, 2007. *Cited on page 1.*

[3] Y. Bai, N. Bandyopadhyay, S. Tsao, S. Slivken, and M. Razeghi, "Room temperature quantum cascade lasers with 27% wall plug efficiency," *Applied Physics Letters*, vol. 98, no. 18, p. 181102, 2011. *Cited on page 2.*

[4] C. Y. Wang, L. Kuznetsova, V. Gkortsas, L. Diehl, F. X. Kaertner, M. A. Belkin, A. Belyanin, X. Li, D. Ham, H. Schneider, *et al.*, "Mode-locked pulses from mid-infrared quantum cascade lasers," *Optics express*, vol. 17, no. 15, pp. 12929–12943, 2009. *Cited on pages 1 and 2.*

[5] H. A. Haus, "Mode-locking of lasers," *IEEE Journal of Selected Topics in Quantum Electronics*, vol. 6, no. 6, pp. 1173–1185, 2000. *Cited on page 1.*

[6] D. Revin, M. Hemingway, Y. Wang, J. Cockburn, and A. Belyanin, "Active mode locking of quantum cascade lasers in an external ring cavity," *Nature communications*, vol. 7, 2016. *Cited on pages 1 and 2.*

[7] S. Barbieri, M. Ravaro, P. Gellie, G. Santarelli, C. Manquest, C. Sirtori, S. P. Khanna, E. H. Linfield, and A. G. Davies, "Coherent sampling of active mode-locked terahertz quantum cascade lasers and frequency synthesis," *Nature Photonics*, vol. 5, no. 5, pp. 306–313, 2011. *Cited on page 2.*

[8] P. Gellie, S. Barbieri, J.-F. Lampin, P. Filloux, C. Manquest, C. Sirtori, I. Sagnes, S. P. Khanna, E. H. Linfield, A. G. Davies, *et al.*, "Injection-locking of terahertz quantum cascade lasers up to 35ghz using rf amplitude modulation," *Optics express*, vol. 18, no. 20, pp. 20799–20816, 2010. *Cited on pages 2 and 14.*

[9] X. Huang, Y. Dikmelik, and C. Gmachl, "Non-uniform lateral current distribution in quantum cascade lasers," *Optics express*, vol. 22, no. 5, pp. 6154–6164, 2014. *Cited on page 3.*

[10] R. Dhar and D. Ban, "Nanoscopic voltage distribution of operating cascade laser devices in cryogenic temperature," *Journal of microscopy*, 2015. *Cited on page 3.*

[11] Y. Xu, R. Gwoziecki, I. Chartier, R. Coppard, F. Balestra, and G. Ghibaudo, "Modified transmission-line method for contact resistance extraction in organic field-effect transistors," *Applied Physics Letters*, vol. 97, no. 6, p. 171, 2010. *Cited on page 5.*

[12] N. Johnston, M. Pan, and S. Kudzma, "An enhanced transmission line method for modelling laminar flow of liquid in pipelines," *Proceedings of the Institution of Mechanical Engineers, Part I: Journal of Systems and Control Engineering*, vol. 228, no. 4, pp. 193–206, 2014. *Cited on page 5.*

[13] C. Yan, Q. J. Wang, L. Diehl, M. Hentschel, J. Wiersig, N. Yu, C. Pflügl, F. Capasso, M. A. Belkin, T. Edamura, *et al.*, "Directional emission and universal far-field behavior from semiconductor lasers with limaçon-shaped microcavity," *Applied Physics Letters*, vol. 94, no. 25, p. 251101, 2009. *Cited on page 5.*

[14] K. Yee, "Numerical solution of initial boundary value problems involving maxwell's equations in isotropic media," *IEEE Transactions on antennas and propagation*, vol. 14, no. 3, pp. 302–307, 1966. *Cited on page 7.*

[15] D. Yang, P. Tong, and X. Deng, "A central difference method with low numerical dispersion for solving the scalar wave equation," *Geophysical Prospecting*, vol. 60, no. 5, pp. 885–905, 2012. *Cited on page 7.*

[16] A. Orlandi and C. R. Paul, "Fdtd analysis of lossy, multiconductor transmission lines terminated in arbitrary loads," *IEEE Transactions on Electromagnetic Compatibility*, vol. 38, no. 3, pp. 388–399, 1996. *Cited on page 8.*

[17] S. Ramo, J. R. Whinnery, and T. Van Duzer, *Fields and waves in communication electronics*. John Wiley & Sons, 2008. *Cited on page 9.*

[18] K. Pillai, "Fringing field of finite parallel-plate capacitors," in *Proceedings of the Institution of Electrical Engineers*, vol. 117, pp. 1201–1204, IET, 1970. *Cited on page 9.*

[19] W. Maineult, L. Ding, P. Gellie, P. Filloux, C. Sirtori, S. Barbieri, T. Akalin, J.-F. Lampin, I. Sagnes, H. Beere, *et al.*, "Microwave modulation of terahertz quantum cascade lasers: a transmission-line approach," *Applied Physics Letters*, vol. 96, no. 2, p. 021108, 2010. *Cited on page 10.*